blood®
Regular Article

RED CELLS, IRON, AND ERYTHROPOIESIS

Bone-derived C-terminal FGF23 cleaved peptides increase iron availability in acute inflammation

Guillaume Courbon,[1] Jane Joy Thomas,[1] Marta Martinez-Calle,[1] Xueyan Wang,[1] Jadeah Spindler,[1] John Von Drasek,[1] Bridget Hunt-Tobey,[1] Rupal Mehta,[1] Tamara Isakova,[1] Wenhan Chang,[2] John W. M. Creemers,[3] Peng Ji,[4] Aline Martin,[1] and Valentin David[1]

[1]Division of Nephrology and Hypertension, Department of Medicine, Center for Translational Metabolism and Health, Institute for Public Health and Medicine, Northwestern University Feinberg School of Medicine, Chicago, IL; [2]Endocrine Research Unit, San Francisco Veterans Affairs Medical Center, University of California San Francisco, San Francisco, CA; [3]Laboratory of Biochemical Neuroendocrinology, KU Leuven, Leuven, Belgium; and [4]Department of Pathology, Northwestern University Feinberg School of Medicine, Chicago, IL

KEY POINTS

- Osteocytes are the main source of Cter-FGF23 peptides in acute inflammation.
- Bone-derived Cter-FGF23 peptides are iron conserving molecules and antagonize BMP-induced hepcidin production.

Inflammation leads to functional iron deficiency by increasing the expression of the hepatic iron regulatory peptide hepcidin. Inflammation also stimulates fibroblast growth factor 23 (FGF23) production by increasing both *Fgf23* transcription and FGF23 cleavage, which paradoxically leads to excess in C-terminal FGF23 peptides (Cter-FGF23), rather than intact FGF23 (iFGF23) hormone. We determined that the major source of Cter-FGF23 is osteocytes and investigated whether Cter-FGF23 peptides play a direct role in the regulation of hepcidin and iron metabolism in response to acute inflammation. Mice harboring an osteocyte-specific deletion of *Fgf23* showed a ~90% reduction in Cter-FGF23 levels during acute inflammation. Reduction in Cter-FGF23 led to a further decrease in circulating iron in inflamed mice owing to excessive hepcidin production. We observed similar results in mice showing impaired FGF23 cleavage owing to osteocyte-specific deletion of *Furin*. We next showed that Cter-FGF23 peptides bind members of the bone morphogenetic protein (BMP) family, BMP2 and BMP9, which are established inducers of hepcidin. Coadministration of Cter-FGF23 and BMP2 or BMP9 prevented the increase in *Hamp* messenger RNA and circulating hepcidin levels induced by BMP2/9, resulting in normal serum iron levels. Finally, injection of Cter-FGF23 in inflamed Fgf23^{KO} mice and genetic overexpression of Cter-Fgf23 in wild type mice also resulted in lower hepcidin and higher circulating iron levels. In conclusion, during inflammation, bone is the major source of Cter-FGF23 secretion, and independently of iFGF23, Cter-FGF23 reduces BMP-induced hepcidin secretion in the liver.

Introduction

Fibroblast growth factor 23 (FGF23) is a phosphate and vitamin D regulating hormone produced in the bone by osteocytes.[1-4] A complex network of classical mediators of bone and mineral metabolism regulates FGF23 production.[5-8] High levels of parathyroid hormone, phosphate, calcitriol, and calcium stimulate *Fgf23* transcription.[6,9-11] Consequently, FGF23 is secreted into the circulation as an intact, biologically active hormone (intact FGF23 [iFGF23]). Nonclassical stimuli also control FGF23 production, including true iron deficiency, inflammation and functional iron deficiency, erythropoietin administration, and acute blood loss.[12-18] However, in these settings, increased FGF23 production is associated with increased proteolytic cleavage to yield FGF23 cleavage peptides that have not been shown to have a biological activity in bone and mineral metabolism.[13,19,20] Although the well-established function of iFGF23 is to maintain normal phosphate homeostasis, there is emerging evidence supporting extrarenal FGF23 targets.[21-23] FGF23-derived cleavage peptides are ineffective in regulating phosphate and vitamin D metabolism, but they may play a role in mediating some of these more recently discovered extrarenal FGF23 functions.

A tightly regulated coupling between FGF23 transcription and downstream proteolytic cleavage results in varying proportions of circulating intact (iFGF23), N-terminal FGF23, and C-terminal (Cter-FGF23) peptides, referred to as total FGF23. O-glycosylation of iFGF23 by GALNT3 at its major 176-RXXR-179 cleavage site prevents proteolytic cleavage.[24] Conversely, phosphorylation at the same site by family with sequence similarity 20, member C (Fam20C) enables cleavage of iFGF23 by proprotein convertases serine kinases.[25-27] The fact that both FGF23 production and cleavage are induced by inflammation, iron deficiency, anemia, and EPO, with minimal impact on circulating iFGF23 levels,[12-18] supports a possible role of FGF23-cleaved peptides under these conditions. Consistent with this hypothesis, we have shown that excess total FGF23 correlated with prevalent anemia, change in hemoglobin (Hb) over time, and development of anemia.[28] FGF23

has also been shown to induce anemia, suggesting that iFGF23 or FGF23-derived peptides might have a direct impact on iron metabolism and/or erythropoiesis.[29]

Increased production of the iron regulatory hormone hepcidin in response to inflammatory cytokines is a major cause of functional iron deficiency and anemia.[30] Hepcidin is the main regulator of plasma iron concentrations, which acts by modulating cellular iron export to plasma and extracellular fluid and, thus, is the principal regulator of iron absorption and its distribution to tissues. During inflammatory conditions, bone morphogenetic proteins (BMP) signaling in hepatocytes increases the secretion of hepcidin,[31-34] which downregulates the iron exporter ferroportin, thus limiting iron entry into the bloodstream from absorptive enterocytes, macrophages, and hepatocytes body stores.

Here, we tested the role of Cter-FGF23 peptides on iron metabolism during acute inflammation. We show that bone represents the major source of Cter-FGF23 peptides during acute inflammation. We also show that furin is the major protease responsible for FGF23 cleavage in response to interleukin-1β (IL-1β) administration. Importantly, we demonstrate that Cter-FGF23 depletion, owing to the genetic deletion of *Fgf23* or *Furin*, aggravates functional iron deficiency in acute inflammation. Finally, we show that exogenous administration and/or genetic overexpression of Cter-FGF23 increases iron bioavailability by antagonizing BMP-dependent hepcidin production. Together, our data show that bone-produced Cter-FGF23 peptides are new iron conserving molecules and that Cter-FGF23 peptides could represent a therapy to alleviate inflammation-induced anemia.

Methods

Animals

A 6-week-old male, wild type (WT), $Fgf23^{KO}$, and Cre-recombinase mice driven by dentin matrix protein 1 promoter ($DMP1^{Cre+}$) were purchased from The Jackson Laboratory. $Fgf23^{flox/flox}$ mice[35] were from the laboratory of W.C. (University of California San Francisco, San Francisco, CA), $Furin^{flox/flox}$ mice[36] were from the laboratory of J.W.M.C. (Center for Human Genetics, KU Leuven, Leuven, Belgium), and $Dmp1^{KO}$ mice were provided by Jian Q. Feng's laboratory (Baylor College of Dentistry at Texas A&M Health Science Center, Dallas, TX). Flox mice were crossed with Dmp1-Cre mice to generate $Fgf23^{flox/flox}$-$Dmp1^{Cre-}$, $Fgf23^{flox/flox}$-$Dmp1^{Cre+}$, $Furin^{flox/flox}$-$Dmp1^{Cre-}$, and $Furin^{flox/flox}$-$Dmp1^{Cre+}$. $Dmp1^{Cre-}$ served as WT littermate controls. We created the Fgf23 conditional transgenic mouse (Cter-$Fgf23^{Dmp1\text{-}cTg}$), as detailed in supplemental Methods, available on the *Blood* website. All experiments were approved by the Northwestern University Institutional Animal Care and Use Committee.

Recombinant proteins

Proteins were purchased and used as detailed in supplemental Data.

Gelatin sponge scaffold implants

Mice were implanted with 5 mm × 5 mm absorbable gelatin sponges (Gelfoam; Pfizer, New York, NY) containing MC3T3-E1 cells stably overexpressing the sequence encoding the aa 179 to 251 Cter-FGF23 peptide or an empty vector (Ctr). Briefly, MC3T3-E1 were seeded on gelatin sponges in vitro in cell culture medium. After 15 hours, the mice were anesthetized, and the sponge was implanted subcutaneously in the mid-dorsal area. Blood and tissues were collected 24 hours after implanting the sponge.

Tissue collection

Tissues were collected and prepared as detailed in supplemental Data.

Biochemistry

Biochemistry assays were performed as detailed in supplemental Data.

Ex vivo tissue secretion

Cortical bones, bone marrow, calvaria, liver, spleen, kidney and heart were harvested from mice and cultured in 6-well plates in optimized minimum essential medium supplemented with 1% fetal bovine serum. Supernatants were collected after 24 hours and secreted cFGF23 and iFGF23 were measured immediately.

Primary cell culture

Primary cells were cultured as previously described[37] and detailed in supplemental Data.

Luciferase assay

MC3T3-E1 cells transfected with a secreted luciferase under the control of the 1.5 Kb promoter of *Fgf23* sequence were cultured as previously described[37,38] and detailed in supplemental Data.

Hepatocyte cell culture

Mouse cell line FL83B hepatocytes (CRL-2390; ATCC, Manassas, VA) were plated at 3.0×10^4 per cm^2 in F-12K medium for 21 days, and then fasted for 16 hours before challenge with OPTI-MEM minimal medium containing 1% fetal bovine serum. FL83B cells were stimulated with 10 ng/mL BMP2/6/9 in presence or absence of 50 ng/mL of Cter-FGF23.

RNA isolation, RT-PCR, and RNA sequencing

RNA was isolated, purified, and expression measured as previously described[12,38,39] and detailed in supplemental Data and supplemental Table 1.

Immunoprecipitation (IP), western blotting, and mass spectrometry

Serum and cell protein extracts were analyzed as detailed in supplemental Data.

Immunohistochemistry

Decalcified mouse tibia paraffin sections (5 μm) were hydrated and treated with unmasking solution and nonspecific site blockade. FGF23 detection was performed using primary antibodies (1:500; Quidel, San Diego, CA), anti-goat secondary antibody, avidin-biotin coupling, and peroxidase revelation (Vector Labs, Burlingame, CA). Images were captured by bright field microscopy (Leica Microsystems, Buffalo Grove, IL).

Statistics

Data analysis was performed with Statistica (TIBCO Software Inc, Palo Alto, CA) using Student *t* test and analysis of variance.

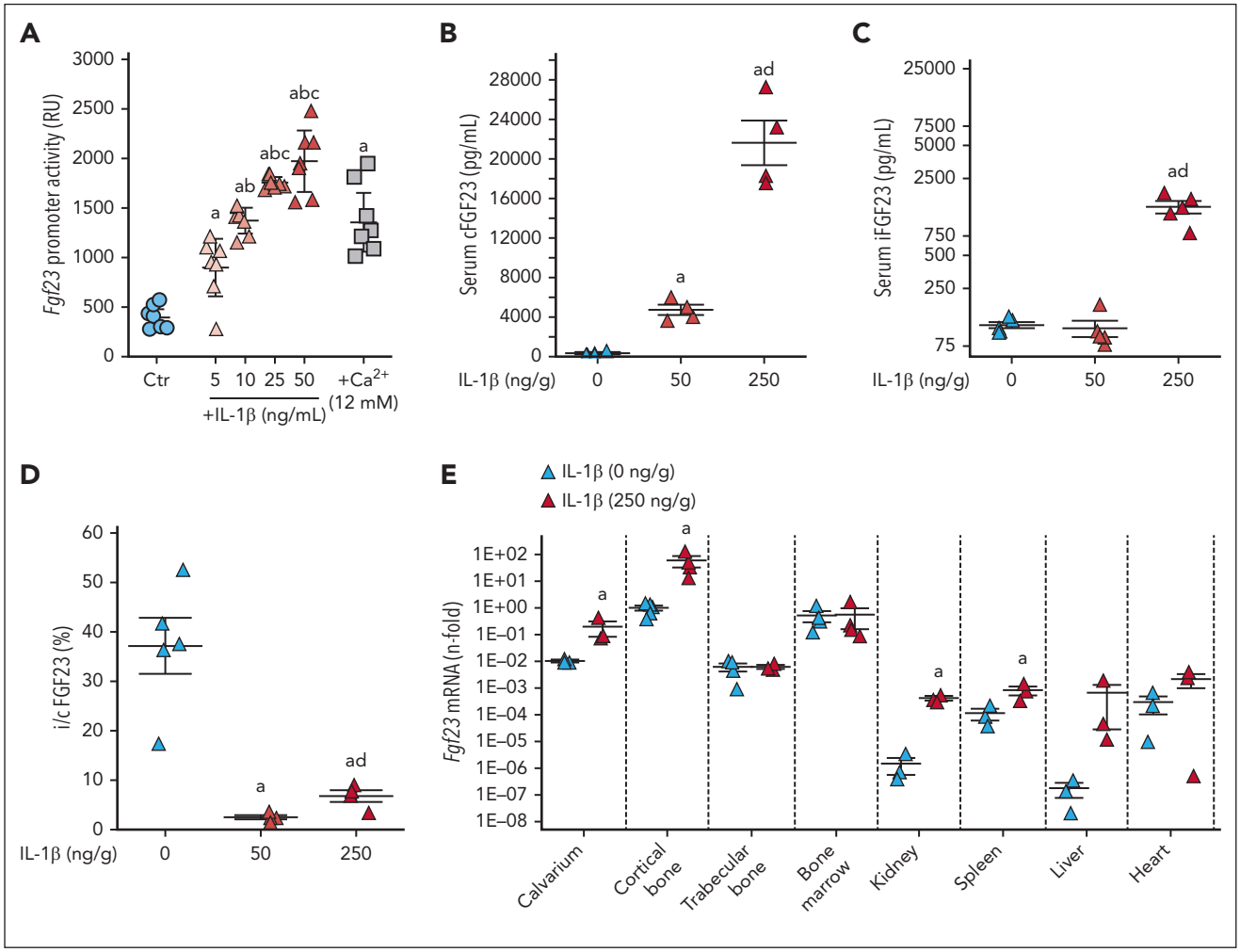

Figure 1. Acute inflammation increases bone FGF23 production. (A) *Fgf23* promoter activity in MC3T3-E1 osteoblasts in response to escalating doses of IL-1β and calcium used as positive control. Serum (B) cFGF23, (C) iFGF23, (D) i/cFGF23, and (E) bone *Fgf23* mRNA expression in 6-week-old WT mice, 6 hours after administration of a single dose of IL-1β. n ≥ 3 per group, $P < .05$ vs (a) 0 (Ctr), (b) 5, (c) 10 ng/mL, and (d) 50 ng/g IL-1β.

The sizes of the different data sets were determined according to the minimal number of animals estimated to reach statistical significance and biological relevance during assessment of the primary outcome for the experiment. Data are presented as mean ± standard error of the mean. P values < 0.05 were considered statistically significant.

Results

Cortical bone is the major contributor of FGF23 production during acute inflammation

Acute inflammation induced by 50 ng/g of IL-1β in mice increases osteoblast/osteocyte *Fgf23* transcription and circulating cFGF23 levels but not iFGF23.[12] *Fgf23* promoter reporter MC3T3-E1 osteoblasts show a dose-dependent increase in *Fgf23* transcription in response to IL-1β (Figure 1A). MC3T3-E1 producing a double tagged FGF23 (red fluorescent protein at the N-terminal and GFP at the C-terminal domain) under the control of *Fgf23* 1.2 Kb promoter also show a time-dependent increase in FGF23 production and secretion of mainly FGF23 fragments (supplemental Videos 1-3). Recent studies have shown that FGF23 can be secreted by other cells/organs under challenge.[18] To determine the major site of production and recruit all available sources of FGF23 in acute inflammation, we administered a 5× higher dose of IL-1β (ie, 250 ng/g) to WT mice. This further increased both cFGF23 and iFGF23, leading to an increase in i/cFGF23 ratio (Figure 1B-D). This higher dose of IL-1β also increased *Fgf23* messenger RNA (mRNA) by 20-fold in calvarium and by ~60-fold in the cortical bone ($P <$ .05), which are enriched in osteocytes. Acute inflammation also modestly increased *Fgf23* expression in kidney, spleen, and liver (Figure 1E). In vitro, short-term organ cultures from WT mice treated in vivo or in vitro with either saline or IL-1β confirmed increased secretion of both c and iFGF23 in the same organs in response to inflammatory stimuli (supplemental Figure 1) and further support that osteocytes are the major source of FGF23 in response to inflammation.

Osteocyte-specific deletion of Fgf23 suppresses FGF23 response to acute inflammation

To further test whether osteocytes are the major source of circulating FGF23 in acute inflammation, we created osteocyte-specific *Fgf23* knockout mice using a Dmp1-Cre recombinase and repeated saline and IL-1β treatments. Vehicle-treated

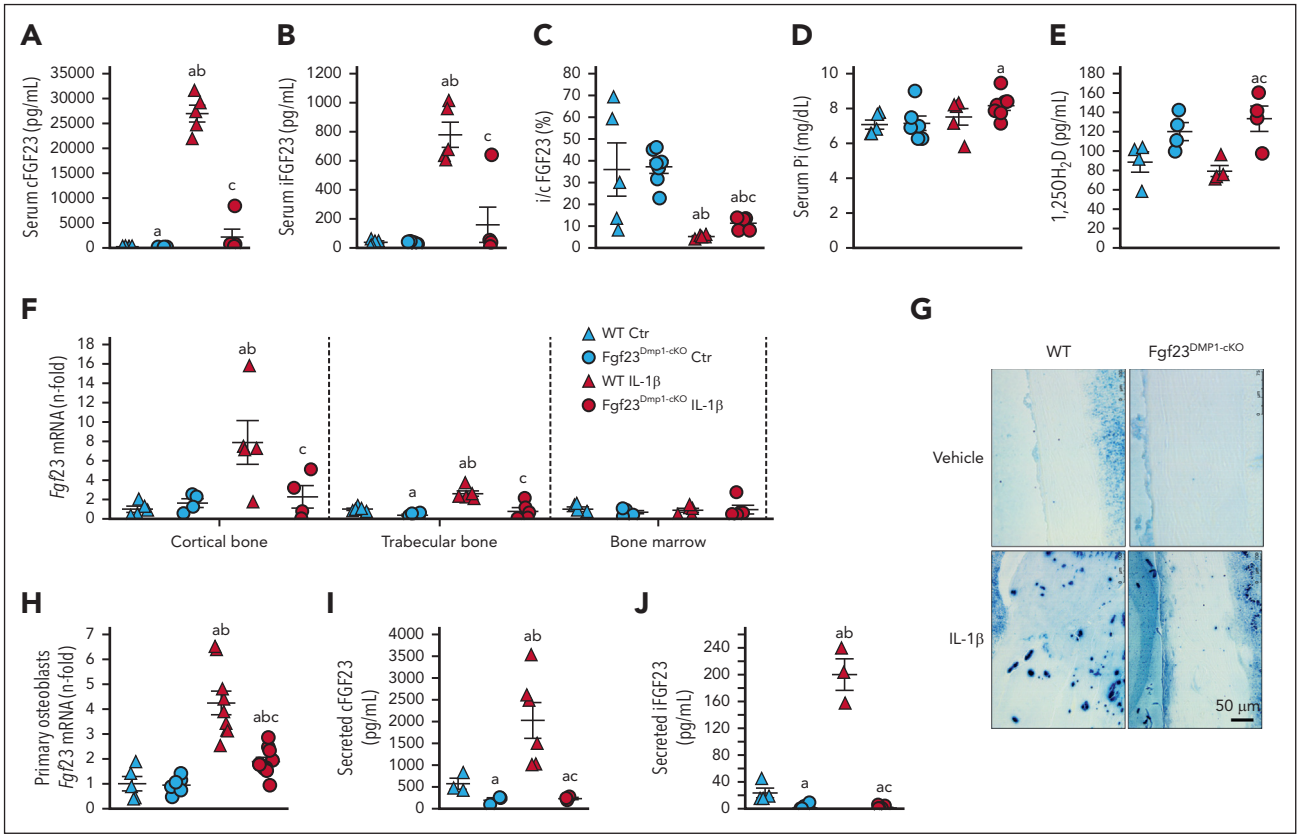

Figure 2. Deletion of *Fgf23* in osteocytes reduces circulating FGF23 in acute inflammation. Serum (A) cFGF23, (B) iFGF23, (C) i/cFGF23, (D) phosphate, (E) 1,25OH_2D, bone (F) *Fgf23* mRNA, and (G) FGF23 protein expression in 6-week-old WT and *Fgf23*$^{Dmp1\text{-}cKO}$ mice 6 hours after administration of a single dose of 250 ng/g IL-1β. n ≥ 5 per group, $P < .05$ vs (a) WT Ctr, (b) *Fgf23*$^{Dmp1\text{-}cKO}$ Ctr (c) WT IL-1β. (H) *Fgf23* mRNA levels and secreted (I) cFGF23 and (J) iFGF23 in primary osteoblast cultures cultured for 3 weeks in osteoblastic medium and treated with saline or 10 ng/mL of IL-1β for 6 hours. n ≥ 3 per group, $P < .05$ vs (a) WT Ctr, (b) *Fgf23*$^{Dmp1\text{-}cKO}$ Ctr (c) WT IL-1β.

Fgf23$^{Dmp1\text{-}cKO}$ mice showed lower circulating levels of cFGF23 but normal iFGF23 levels. In acute inflammation, *Fgf23*$^{Dmp1\text{-}cKO}$ mice secreted a dramatically lower quantity of both c and iFGF23 than that of WT littermates (−92% of circulating cFGF23% and −80% of iFGF23), leading to a slight increase in i/c FGF23 ratio and a mild increase in serum phosphate and calcitriol levels (Figure 2A-E). Inflammation increased *Fgf23* mRNA in the cortical bone of WT but not of *Fgf23*$^{Dmp1\text{-}cKO}$ mice (Figure 2F). Immunohistochemistry showed increased FGF23 in the cortical bone of IL-1β-treated WT but not in IL-1β-treated *Fgf23*$^{Dmp1\text{-}cKO}$ mice (Figure 2G). Of note, IL-1β increased neutrophil count similarly in WT and *Fgf23*$^{Dmp1\text{-}cKO}$ mice (supplemental Figure 2). Primary osteoblasts isolated from the cortical bone of WT and *Fgf23*$^{Dmp1\text{-}cKO}$ mice showed increased *Fgf23* mRNA and supernatant c and iFGF23 levels in response to IL-1β in WT but not in *Fgf23*$^{Dmp1\text{-}cKO}$ cells (Figure 2H-J). Together, these data show that mature osteoblasts/osteocytes are the main cells producing FGF23 in response to inflammation.

Increased furin expression causes cFGF23 excess in acute inflammation

To determine the sequence of events leading to excess FGF23 in acute inflammation, we assessed the hourly response to a single injection of IL-1β in WT mice for 6 hours. IL-1β increased *Fgf23* mRNA in the cortical bone as early as 1 hour after injection (Figure 3A), followed by an increase in serum cFGF23 levels with a maximum peak at 5 hours (Figure 3B). Levels of iFGF23 followed the same pattern, albeit at lower levels (Figure 3C). i/cFGF23 ratio was reduced 2 hours after injection (Figure 3D) and remained low until 6 hours, suggesting early modifications of FGF23 cleavage. IP of FGF23 in serum using antibodies directed against a C-terminal motif of FGF23 confirmed the presence of iFGF23 and cleaved peptides, at predicted sizes (Figure 3E). The expression of *Galnt3*, which protects FGF23 from cleavage, was reduced in the cortical bone only after 4 hours (Figure 3F), and the expression of *Fam20c*, which promotes FGF23 cleavage, peaked at 3 hours after IL-1β injection (Figure 3G). Six hours after IL-1β injection, out of the 9 different proteases predicted to recognize the FGF23 cleavage site, we observed a nonsignificant increase in *Pcsk2* expression in the cortical bone and a significant increase in *Furin* (supplemental Figure 3). In contrast with late modifications in *Galnt3* and *Fam20c* expression, *Furin* mRNA increased as early as 1 hour after IL-1β injection, coinciding with the acute increase in cFGF23 levels (Figure 3H). Given that FGF23 is mostly produced as FGF23 cleaved peptides in acute inflammation (supplemental Videos 1-3), we tested whether cleavage of FGF23 occurs before or after secretion. Bone explants from *Fgf23*^{KO} mice devoid of endogenous FGF23 production and treated with exogenous iFGF23 and IL-1β showed that only a small percentage of iFGF23 was cleaved in response to IL-1β (Figure 3I-K). This suggests that, in acute inflammation, FGF23 peptides result from intracellular cleavage by furin in osteocytes and are subsequently secreted.

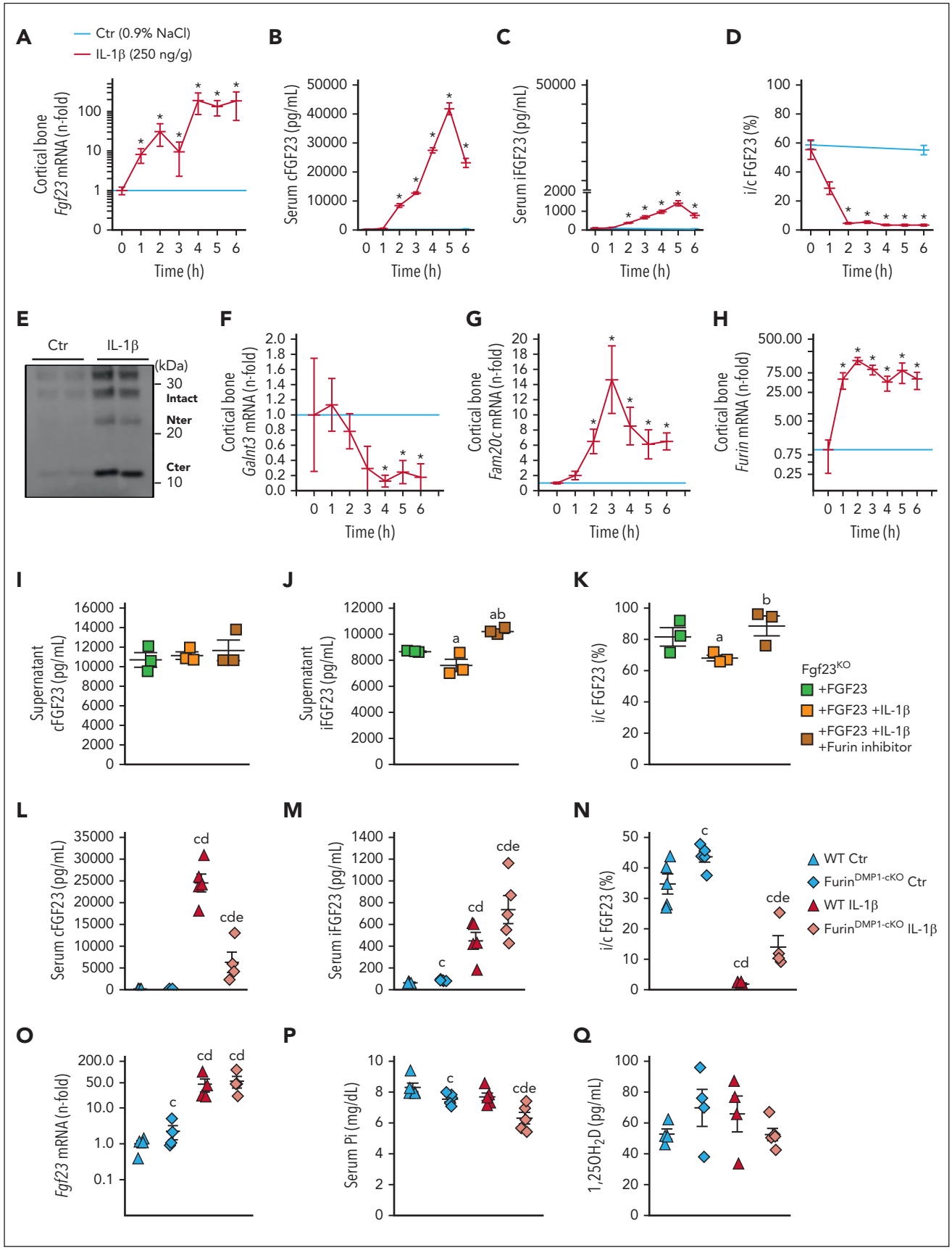

Figure 3. FGF23 cleavage by furin in osteocytes contributes to a time dependent secretion of FGF23 cleaved peptides. (A) Cortical bone *Fgf23* mRNA, serum (B) cFGF23, (C) iFGF23, (D) i/cFGF23, (E) IP/WB of circulating FGF23 peptides, and cortical bone mRNA expression of (F) *Galnt3*, (G) *Fam20c* and (H) *Furin* in 6-week-old WT mice

Accordingly, osteocyte-specific *Furin* knockout mice showed a reduced amount of serum cFGF23 levels in response to acute inflammation, compared with that of IL-1β-treated WT littermates, and a further increase in iFGF23 levels, despite a similar increase in *Fgf23* transcription, lower phosphate, and normal calcitriol levels (Figure 3L-Q). Administration of IL-1β resulted in a similar increase in neutrophils in both WT and $Furin^{Dmp1\text{-}cKO}$ mice (supplemental Figure 4A). As a result of reduced *Furin* expression in bone and increased iFGF23 levels, IL-1β-treated $Furin^{Dmp1\text{-}cKO}$ mice showed an increase in phosphaturia (supplemental Figure 4C). We also observed a reduction in Hb levels in inflamed $Furin^{Dmp1\text{-}cKO}$ mice, likely owing to an independent role of *Furin* on inflammation-driven hemolysis (supplemental Figure 4D).

FGF23 peptides reduce hepdicin secretion and increase iron bioavailability during inflammation

IL-1β administration to WT mice induces functional iron deficiency, leading to a time dependent decrease in circulating iron and transferrin saturation (TSAT) (Figure 4A-B). These expected effects are mainly because of increased hepatic production of the iron regulatory hormone hepcidin, encoded by *Hamp*, which blocks cellular iron export by binding to ferroportin (Figure 4C-E).[40] Consequently, transcription of bone marrow erythroferrone (*Erfe*), a hormone that inhibits hepcidin production, increases (Figure 4F).[41] $Fgf23^{Dmp1\text{-}cKO}$ mice, which produced ~90% less cFGF23 during inflammation, showed a further reduction of serum iron and TSAT in response to IL-1β administration, owing to a surprising increase in hepatic *Hamp* and circulating hepcidin levels that occurred despite a further increase in *Erfe*, compared with that of WT littermates (Figure 4G-K). A similar effect was observed in response to inflammation induced by heat-killed Brucella abortus particles (supplemental Figure 5A-G). Impaired FGF23 cleavage in $Furin^{Dmp1\text{-}cKO}$ mice also further increased *Hamp* and hepcidin in acute inflammation, leading to further reductions in serum iron and TSAT (Figure 4L-O), despite a further increase in *Erfe* (supplemental Figure 4E), suggesting that Cter-FGF23 cleaved peptides increase iron bioavailability by suppressing hepcidin production independently of erythroferrone.

Cter-FGF23 regulates iron metabolism independently of iFGF23 signaling

To further investigate whether bone-produced Cter-FGF23 regulates iron metabolism, we created a Cter-*Fgf23* conditional transgenic mouse overexpressing Cter-*Fgf23* in osteocytes (*Cter-*$Fgf23^{Dmp1\text{-}cTg}$). *Cter-*$Fgf23^{Dmp1\text{-}cTg}$ mice showed a dramatic increase in circulating total cFGF23 and only a modest increase in iFGF23 levels, confirming that these mice secrete mainly Cter-FGF23 peptides (Figure 5A-C). Importantly, serum phosphate levels were normal compared with that of WT littermates (Figure 5D). Excess Cter-FGF23 reduced serum hepcidin levels, leading to increases in serum iron and TSAT (Figure 5E-G). Hb levels also increased in *Cter-*$Fgf23^{Dmp1\text{-}cTg}$ mice (Figure 5H), likely because of increased iron bioavailability. Cter-FGF23-treated WT mice show reduced liver *Hamp* expression and circulating hepcidin levels, increased serum iron and TSAT, and normal phosphate levels (Figure 5I-M), despite normal *Erfe* expression (supplemental Figure 5H). In contrast, animals with a primary increase in iFGF23, such as hypophosphatemic $Dmp1^{KO}$ mice, show unchanged serum iron, TSAT, and Hb compared with that of WT littermates, further suggesting that iFGF23 is not involved in systemic iron regulation (Figure 5N-S). Administration of Cter-FGF23 peptides to $Fgf23^{KO}$ mice, devoid of endogenous FGF23, did not reduce serum hepcidin, likely owing to the confounding effects of hyperphosphatemia and hypervitaminosis D on hepcidin secretion.[42,43] However, administration of Cter-FGF23 peptides prevented the induction of liver *Hamp* expression and circulating hepcidin levels by inflammation and maintained serum iron and TSAT at normal levels compared with $Fgf23^{KO}$ littermates treated with IL-1β alone (Figure 5T-Z). This further demonstrates that Cter-FGF23 peptides do not compete with iFGF23 signaling and act via a fibroblast growth factor receptor–independent mechanism to reduce hepcidin.

Cter FGF23 peptides prevent BMP2- and BMP9-dependent hepcidin secretion

BMP2 and BMP6 are the major hepcidin regulators and stimulate its expression through BMPR/Smad 1/5/9 mechanism.[38,44-46] BMP9 is the most potent inducer of hepcidin in vitro, but its role is disputed in vivo.[31] In WT mice, circulating levels of BMP2 increase and peak as early as 1 hour after IL-1β injection, whereas BMP9 levels peak only at 4 hours (Figure 6A-B). An equivalent enzyme-linked immunosorbent assay currently does not exist to measure circulating BMP6 levels. In the liver, *Bmp2* and *Bmp9* mRNA were increased as early as 1 hour after IL-1β injection, and *Bmp2*, *Bmp6*, and *Bmp9* mRNA were all increased by 6 hours (Figure 6C-F; supplemental Figure 5I-J). Injection of BMP2,6,9 to WT mice increased liver *Hamp* and circulating hepcidin levels, leading to reductions in serum iron and TSAT and normal phosphate levels (Figure 6G-K). Cter-FGF23 cotreatment partially prevented the effects induced by BMP2 and BMP9 but did not antagonize the effects of BMP6. In parallel, we implanted WT mice with subcutaneous scaffolds containing cells overexpressing Cter-FGF23 peptides or empty plasmid. Injection of BMP2/6/9 in these mice showed a similar response to that of mice coinjected with Cter FGF23 and BMPs (supplemental Figure 5K-O). We also treated *Cter-*$Fgf23^{Dmp1\text{-}cTg}$ mice with BMP2/9 and show that overexpression of Cter-FGF23 reduced hepcidin induction by BMP2/9 (supplemental Figure 5P-S). We further confirmed these results in vitro by treating FL83B immortalized hepatocytes with BMP2/6/9, in the presence or absence of Cter-FGF23 (Figure 6L). To determine binding partners of Cter-FGF23 peptides, we treated cultured osteoblasts collected from $Fgf23^{KO}$ mice with exogenous Cter-FGF23 peptides for 2 hours and performed IP/MS analyses after treatment. We identified binding peptide sequences

Figure 3 (continued) up to 6 hours after administration of a single dose of 250 ng/g IL-1β. Supernatant (I) cFGF23, (J) iFGF23 and (K) i/cFGF23 in 24 hours cultures of bone explants from $Fgf23^{KO}$ mice treated with recombinant murine iFGF23 (10 ng/mL) and IL-1β (10 ng/mL) and furin inhibitor (0 or 15 μg/mL). Serum (L) cFGF23, (M) iFGF23, (N) i/cFGF23, (O) bone *Fgf23* mRNA, (P) serum phosphate, and (Q) $1,25OH_2D$ in 6-week-old WT and $Furin^{Dmp1\text{-}cKO}$ mice 6 hours after administration of a single dose of 250 ng/g IL-1β. n ≥ 3 per group, $P < .05$ vs (*) Ctr, (a) $Fgf23^{KO}$ + FGF23, (b) $Fgf23^{KO}$ + FGF23 + IL-1β, (c) WT Ctr, (d) $Furin^{Dmp1\text{-}cKO}$ Ctr, (e) WT IL-1β.

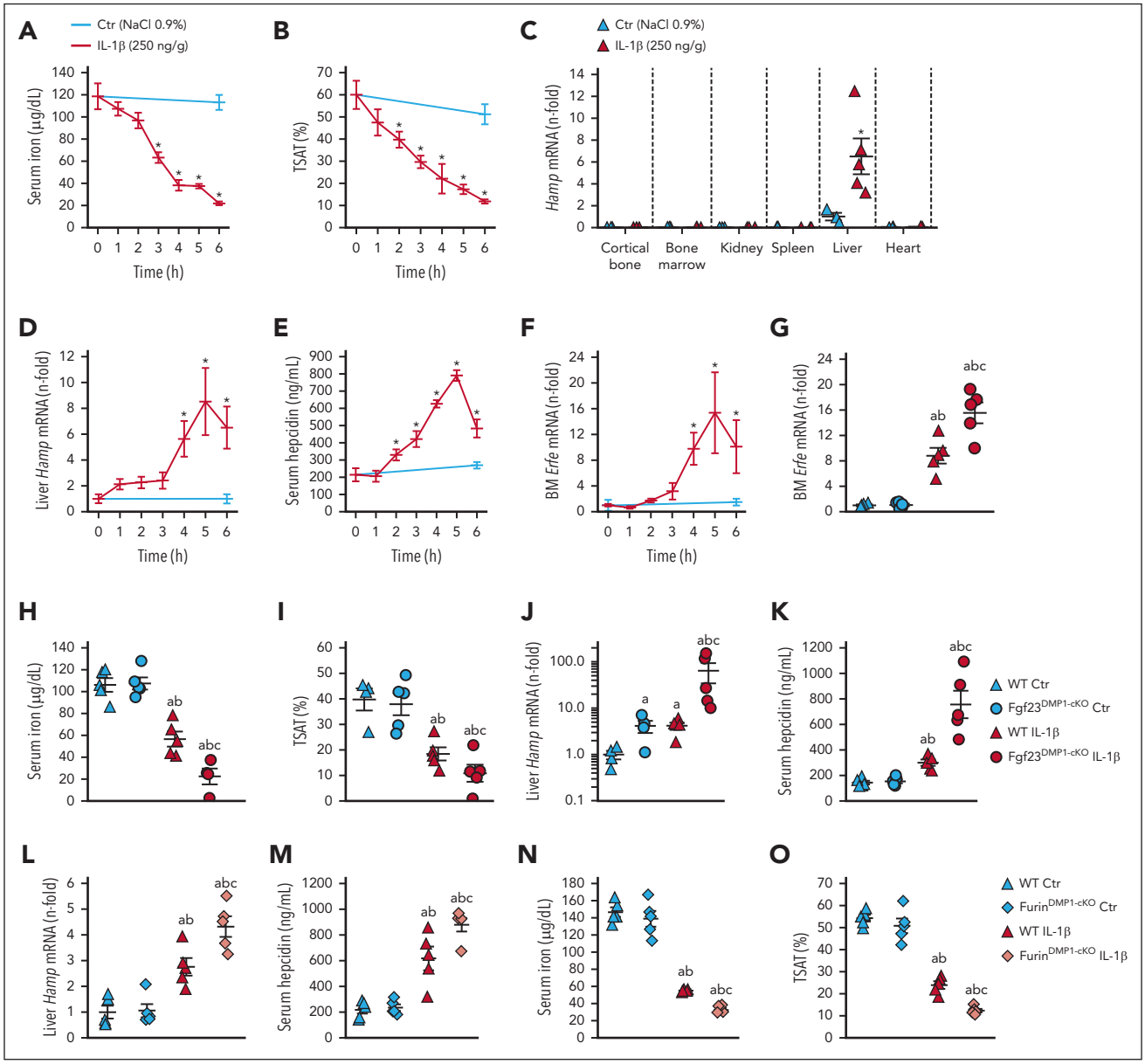

Figure 4. Impaired FGF23 cleavage aggravates functional iron deficiency in acute inflammation. Time course of serum (A) iron and (B) TSAT, (C) *Hamp* mRNA expression in selected organs, (D) liver *Hamp* mRNA expression, (E) serum hepcidin, and (F) bone marrow *Erfe* mRNA expression in 6-week-old WT mice, 6 hours after administration of a single dose of 250 ng/g IL-1β. (G) bone marrow *Erfe* mRNA expression and serum (H) iron and (I) TSAT, (J) liver *Hamp* mRNA expression and serum (K) hepcidin in 6-week-old WT and $Fgf23^{Dmp1\text{-}cKO}$ mice 6 hours after administration of a single dose of 250 ng/g IL-1β. (L) Liver *Hamp* mRNA expression, serum (M) hepcidin, (N) iron and (O) TSAT in 6-week-old WT and $Furin^{Dmp1\text{-}cKO}$ mice 6 hours after administration of a single dose of 250 ng/g IL-1β. n ≥ 5 per group. $P < .05$ vs (*) Ctr, (a) WT Ctr, (b) *cKO* Ctr, (c) WT IL-1β.

belonging to BMP2 and BMP9 (Table 1). To study the putative interactions of BMP2 and BMP9 with Cter-FGF23, we used the AlphaFold structure of murine iFGF23 (Q9EPC2) (Figure 6M) and AlphaFold2 to isolate Cter-FGF23 peptide structure (Figure 6N) and the most likely predicted structure of the isolated peptide (Figure 6O). We also obtained the structure of murine BMP2 (P21274) and BMP9 (Q9WV56) from the AlphaFold Protein Structure Database and used pyDock and UCSF ChimeraX 1.3 to simulate and visualize docking between Cter-FGF23 peptides and BMPs. BMP2 is a dimeric protein, and 2 known receptor-binding motifs have been identified in the BMP2 ligand. A large epitope 1 (wrist) is a high-affinity binding site for BMPR-IA, and a smaller epitope 2 (knuckle) is a low-affinity binding site for BMPR-II (Figure 6P). Cter-FGF23 peptides are predicted to bind to 2 regions in the monomeric BMP2, including BMPR-II binding site (not shown), or to the dimeric BMP2 (Figure 6Q). We obtained similar predicted interactions between BMP9 and Cter-FGF23, with a high-affinity binding in the BMP9/BMPR-II region (Figure 6R). We also observed similar interactions with the least likely AlphaFold2 predicted models of Cter-FGF23 (not shown). Accordingly, $Cter\text{-}Fgf23^{Dmp1\text{-}cTg}$ mice did not show increased hepcidin secretion in response to IL-1β administration and showed a reduction in the SMAD/BMP pathway activation in liver RNA-seq analyses, despite a slight increase in both *Bmp2* and *Bmp6* transcripts in IL-1β-treated

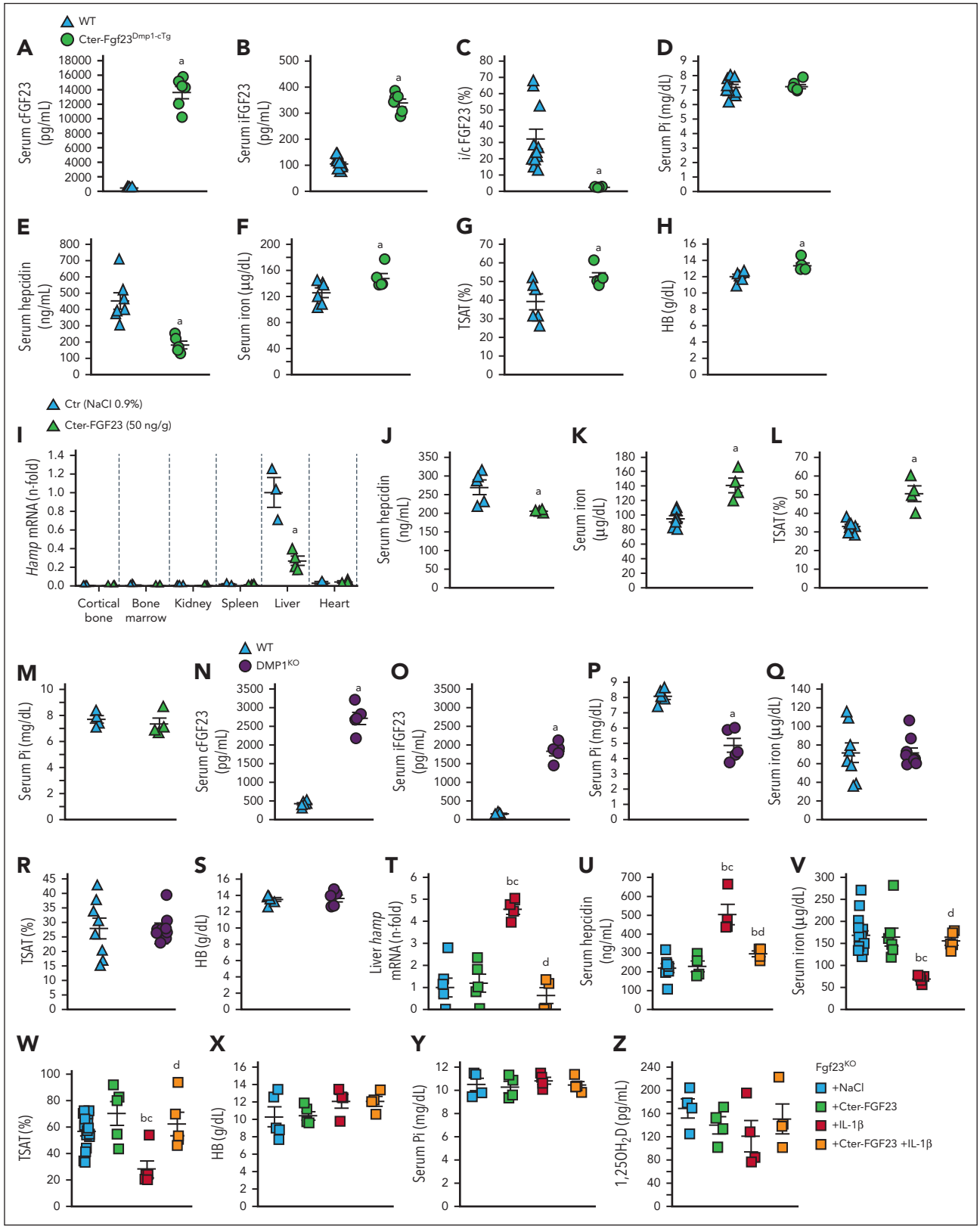

Figure 5. Cter-FGF23 peptides directly regulate iron metabolism in mice. Serum (A) cFGF23, (B) iFGF23, (C) i/cFGF23 ratio, (D) phosphate, (E) hepcidin, (F) iron, (G) TSAT, and (H) Hb in 6-week-old WT and *Cter-Fgf23*$^{Dmp1\text{-}cTg}$ mice. Liver (I) *Hamp* mRNA expression, serum (J) hepcidin, (K) iron and (L) TSAT and (M) phosphate in 6-week-old WT mice 6 hours after administration of a single dose of 50 ng/g Cter-FGF23. Serum (N) cFGF23, (O) iFGF23, (P) phosphate, (Q) iron, (R) TSAT, and (S) Hb in 6-week-old WT and *Dmp1*^{KO} mice. Liver (T) *Hamp* mRNA, serum (U) hepcidin, (V) iron and (W) TSAT, (X) Hb, (Y) phosphate and (Z) 1,25OH_2D in 6-week-old *FGF23*^{KO} mice 6 hours after administration of a single dose of Cter-FGF23 (50 ng/g), IL-1β (250 ng/g), or both. n ≥ 5 per group. $P < .05$ vs (a) WT/Ctr, (b) *Fgf23*^{KO} + NaCl, (c) *Fgf23*^{KO} + Cter-FGF23, (d) *Fgf23*^{KO} + IL-1β.

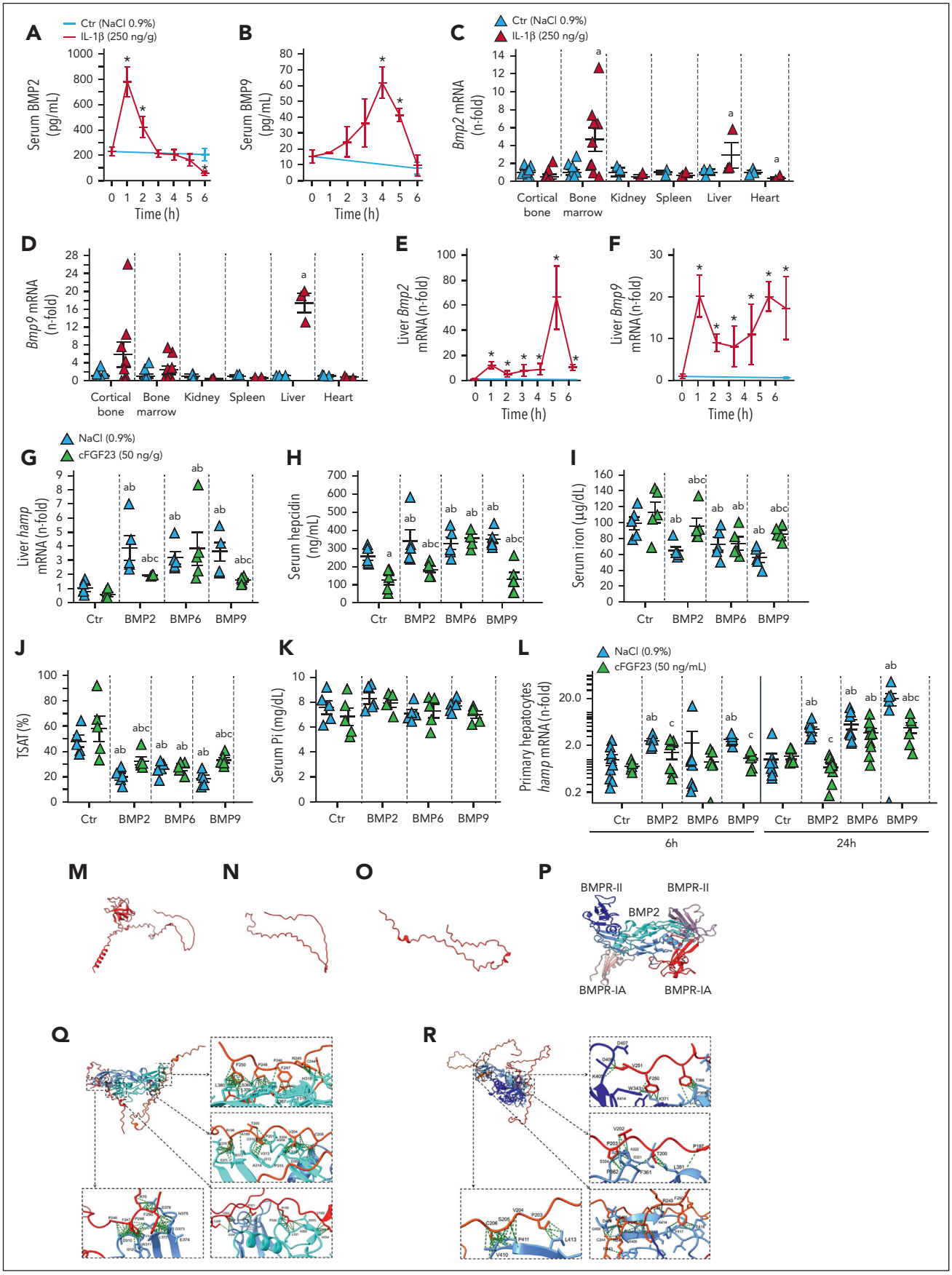

Figure 6.

Table 1. IP/LC-MS analyses of target proteins bound to FGF23 in differentiated mouse osteoblasts treated with iFGF23 or Cter-FGF23 for 2 hours

Peptide sequences	Target protein	Exclusive spectrum count	
		iFGF23	Cter-FGF23
VNFEDIGWDSWIIAPKEYDAYECKGGCFFPLADDVTPTKHAIVQTLVHLK	BMP2	0	3
ACCVPTELSAISMLYLDENEKVVLKNYQDMVVEGCGCR	BMP2	0	11
VNFEDIGWDSWIIAPKEYDAYECKGGCFFPLADDVTPTKHAIVQTLVHLK	BMP9	0	27
ACCVPTELSAISMLYLDENEKVVLKNYQDMVVEGCGCR	BMP9	0	41

Cter-Fgf23$^{Dmp1\text{-}cTg}$ mice vs IL-1β-treated WT (supplemental Figure 6). Taken together, these data suggest that Cter-FGF23 antagonizes BMP2 and BMP9-dependent stimulation of hepcidin by preventing the binding of BMP2 and BMP9 to BMP receptors.

Discussion

Circulating FGF23 levels are regulated by a balance between *Fgf23* transcription and FGF23 cleavage.[12,13] Associations between excess FGF23 and inflammation have generated interest in possible new functions for iFGF23 and FGF23-derived peptides. Indeed, we and others have shown that increased iFGF23 promotes inflammation.[21,47] We also showed that inflammation is a potent driver of FGF23 production.[12,39] In contrast with hyperphosphatemia, hyperparathyroidism, and other acquired or genetic conditions leading to increased iFGF23,[1-4] acute inflammation triggers an increase in FGF23 production and a concomitant increase in FGF23 cleavage. This leads to a dramatic increase in circulating total FGF23, assessed by increased cFGF23, but only a modest increase in iFGF23.[12,39] The mechanisms leading to excess FGF23 cleaved peptides remain largely undefined, and the biological significance of excess Cter-FGF23 has been under debate, considering that these peptides are devoid of a phosphaturic effect. Here, we show that both Cter-FGF23 and N-terminal FGF23 peptides are secreted from cells producing iFGF23 in response to IL-1β treatment. We demonstrate that bone is the major source of FGF23 production during acute inflammation. Most importantly, we also show that bone-produced Cter-FGF23 directly regulates iron metabolism, increases iron bioavailability, and prevents severe hypoferremia during acute inflammation by antagonizing BMP-induced hepcidin production.[48]

FGF23 is mainly secreted from osteocytes and osteoblasts in bone.[1-4] Recent published evidence[14,18,49-52] shows that, in addition to bone, intact and cleaved FGF23 are also produced by bone marrow. Several reports suggest that inflammation-induced FGF23 excess might be the result of increased FGF23 secretion by multiple organs.[53,54] In this study, we show that bone, the main source of circulating FGF23 in physiological conditions, is also the main contributor to FGF23 production in acute inflammation. Indeed, bone-specific deletion of *Fgf23* leads to 80% to 90% reduction in both intact and cFGF23. In this study, we provide an active mechanism leading to excess Cter-FGF23 during inflammation. FGF23 peptides are generated by increased post-transcriptional cleavage of iFGF23 176-RXXR-179 site.[55] O-glycosylation at the cleavage site by polypeptide N-acetylgalactosaminyl-transferase 3 (GALNT3) protects FGF23 from cleavage and ensures its secretion,[25,56] whereas phosphorylation at the cleavage site by Fam20C inhibits O-glycosylation and promotes cleavage.[27] Previous studies have shown that multiple proteases have the capacity to subsequently cleave FGF23 in vitro and in vivo.[26,27,57-59] Furin-like proteases have been previously described as the most likely candidates responsible for FGF23 cleavage but the exact enzyme has not been clearly identified. In addition to increased *Fgf23* transcription in osteocytes, we show that inflammation leads to a reduction of *Galnt3* expression that is paralleled by an increase in *Fam20c* expression and a very acute and sustained increase in *Furin* expression. Together, this represents a strong combination toward a rapid increase in FGF23 cleavage directly after it is produced. We further found that in acute inflammation, deletion of furin prevents the sharp increase in the levels of Cter-FGF23, suggesting that the coordinated increases in the expression of *Fgf23* and *Furin* are largely responsible for excess Cter-FGF23 in response to inflammation. Although furin can process both intracellular and extracellular proteins, our data suggest that iFGF23 is cleaved intracellularly before secretion.

The dramatic increase in both *Fgf23* transcription and FGF23 cleavage questions the physiological need for increased *Fgf23* transcription in inflammatory conditions. Until now, the possibility for physiological and pathological effects of FGF23-derived peptides remained uncertain, because most studies focused on the function of iFGF23 only. The C-terminal domain is unique to each member of the FGF family. For FGF23, it allows binding to its coreceptor alpha klotho,[60-62] which is involved in the phosphaturic response to iFGF23. As such, a few

Figure 6. Cter-FGF23 peptides antagonize BMP2/9-induced hepcidin secretion. Time course of serum (A) BMP2 and (B) BMP9, mRNA expression of (C) *Bmp2* and (D) *Bmp9* in selected organs and time course mRNA expression of liver (E) *Bmp2* and (F) *Bmp9* in 6-week-old WT mice, 6 hours after administration of a single dose of 250 ng/g IL-1β. Liver (G) *Hamp* mRNA expression and serum (H) hepcidin, (I) iron and (J) TSAT and (K) phosphate in 6-week-old WT mice 6 hours after administration of a single dose of 50 ng/g Cter-FGF23, 10 ng/g BMP (2, 6 or 9), or both. n ≥ 5 per group. Expression of (L) *Hamp* mRNA in primary hepatocytes treated with Cter-FGF23 (50 ng/mL), 10 ng/mL BMP (2, 6 or 9) or both for 6 and 24 hours. n ≥ 5 per group. $P < .05$ vs (*) Ctr T0, (a) Ctr NaCl, (b) Ctr Cter-FGF23, (c) BMP (2, 6, 9). (M) iFGF23 predicted 3D structure, (N) Cter-FGF23 isolated from panel M, (O) predicted AlphaFold2 Cter-FGF23 structure (model 0), (P) BMP2 dimer (blue) binding BMPR-II (purple) and BMPR-IA (red), (Q) Interaction of 2 molecules of Cter-FGF23 with a dimeric BMP2 at the BMPR-II site, (R) Interaction of 2 molecules of Cter-FGF23 with a dimeric BMP9.

reports have suggested that Cter-FGF23 peptides might antagonize iFGF23 signaling; however, these studies relied on the administration of Cter-FGF23 of human origin to rodents,[63-66] which might elicit different cross-species effects. However, in this study, neither the administration of murine Cter-FGF23 to WT or hyperphosphatemic animals devoid of endogenous *Fgf23* production nor the bone conditional overexpression of Cter-FGF23 led to modifications of circulating phosphate levels, suggesting that Cter-FGF23 peptides do not interfere with iFGF23 signaling and iFGF23-mediated regulation of phosphate homeostasis. Excess FGF23 might be a causal factor for anemia and was associated with prevalent anemia, change in Hb over time, and development of anemia in patients with chronic kidney disease.[28] FGF23 has also been shown to induce anemia,[29] but these studies did not differentiate between iFGF23 and total cFGF23. In this study, to our knowledge, we show for the first time that Cter-FGF23 is a direct and powerful regulator of iron metabolism. Using *Dmp1*^{KO} mice, an established model of hypophosphatemic rickets with primary iFGF23 excess, we excluded bone-produced iFGF23 as a causative factor for perturbed iron metabolism or anemia, because these mice show normal iron and Hb levels. Genetic deletion of *Fgf23* from bone, that leads to a decline in both Cter and iFGF23 levels, paradoxically aggravated iron deficiency in mice exposed to IL-1β injections, and we replicated these effects in mice harboring a genetic deletion of *Furin* in bone that prevents FGF23 cleavage and results in inadequately low levels of Cter-FGF23 in response to inflammation. Together these data suggest that increased Cter-FGF23 production is an adaptive response to prevent severe hypoferremia and aggravated anemia in inflammation.

Increased production of hepcidin in response to inflammatory cytokines is a major cause of functional iron deficiency and anemia.[67] BMP signaling in hepatocytes increases the secretion of hepcidin.[31-33] These findings show that Cter-FGF23 directly regulates iron metabolism by reducing hepcidin secretion by acting as a BMP antagonist. Whether Cter-FGF23 has other physiological functions remains to be studied. Similarly, as Cter-FGF23 peptides are only minimally increased during chronic inflammation,[12] it remains to be determined whether this increase is sufficient to reduce hepcidin and increase iron bioavailability in chronic conditions.

In multiple studies, total cFGF23, rather than iFGF23, is associated with adverse outcomes, including anemia, change in Hb over time, and mortality.[28,68] Our studies propose an active and iFGF23-independent mechanism for the iron conserving properties of bone-derived Cter-FGF23 peptides. Our results suggest that the coordinated increase in FGF23 production and cleavage in osteocytes is an initial adaptive response to alleviate the burden of anemia of inflammation and, ultimately, support an active coupling between the regulation of iron and phosphate metabolisms.

Acknowledgments

This manuscript used services from the Northwestern Proteomics Core and NUseq Core.

This study was supported by grants from National Institutes of Health to V.D. (R01DK102815, R01DK114158, R01DK132657), A.M. (R01DK101730, R01DK131046, R01DK132342), and P.J. (R01-DK124220, R01-HL148012, R01-HL150729).

Authorship

Contribution: V.D. designed the study; G.C., A.M., and V.D. drafted the manuscript; and all authors contributed to data acquisition and data interpretation, revised the manuscript, reviewed and approved the final version of the manuscript.

Conflict-of-interest disclosure: V.D. received research funding from Akebia and has received research funding from Vifor Pharma and consulting honoraria from Keryx Biopharmaceuticals, Vifor Pharma, Luitpold, and Amgen, outside of the submitted work. The remaining authors declare no competing financial interests.

ORCID profiles: G.C., 0000-0002-2410-4571; W.C., 0000-0001-6583-7176; P.J., 0000-0002-8849-3625; A.M., 0000-0002-0144-9294; V.D., 0000-0001-9527-2364.

Correspondence: Valentin David, Division of Nephrology and Hypertension, Department of Medicine, Center for Translational Metabolism and Health, Institute for Public Health and Medicine, Northwestern University Feinberg School of Medicine, Searle 10th floor, 320 East Superior St, Chicago, IL 60611; email: valentin.david@northwestern.edu.

Footnotes

Submitted 26 October 2022; accepted 6 April 2023; prepublished online on *Blood* First Edition 13 April 2023. https://doi.org/10.1182/blood.2022018475.

RNA-seq data were submitted to the Gene Expression Omnibus (GEO) repository and are accessible under accession number GSE227268.

All data associated with this study are presented in the article. Materials and protocols are available upon demand.

The online version of this article contains a data supplement.

There is a *Blood* Commentary on this article in this issue.

The publication costs of this article were defrayed in part by page charge payment. Therefore, and solely to indicate this fact, this article is hereby marked "advertisement" in accordance with 18 USC section 1734.

REFERENCES

1. Liu S, Zhou J, Tang W, Jiang X, Rowe DW, Quarles LD. Pathogenic role of Fgf23 in Hyp mice. *Am J Physiol Endocrinol Metab*. 2006;291(1):E38-E49.

2. Feng JQ, Ward LM, Liu S, et al. Loss of DMP1 causes rickets and osteomalacia and identifies a role for osteocytes in mineral metabolism. *Nat Genet*. 2006;38(11):1310-1315.

3. Pereira RC, Juppner H, Azucena-Serrano CE, Yadin O, Salusky IB, Wesseling-Perry K. Patterns of FGF-23, DMP1, and MEPE expression in patients with chronic kidney disease. *Bone*. 2009;45(6):1161-1168.

4. Riminucci M, Collins MT, Fedarko NS, et al. FGF-23 in fibrous dysplasia of bone and its relationship to renal phosphate wasting. *J Clin Invest*. 2003;112(5):683-692.

5. Bonewald LF, Wacker MJ. FGF23 production by osteocytes. *Pediatr Nephrol*. 2013;28(4):563-568.

6. David V, Dai B, Martin A, Huang J, Han X, Quarles LD. Calcium regulates FGF-23 expression in bone. *Endocrinology*. 2013;154(12):4469-4482.

7. Ito N, Findlay DM, Anderson PH, Bonewald LF, Atkins GJ. Extracellular phosphate modulates

the effect of 1alpha,25-dihydroxy vitamin D3 (1, 25D) on osteocyte like cells. *J Steroid Biochem Mol Biol*. 2013;136:183-186.

8. Shimada T, Kakitani M, Yamazaki Y, et al. Targeted ablation of Fgf23 demonstrates an essential physiological role of FGF23 in phosphate and vitamin D metabolism. *J Clin Invest*. 2004;113(4):561-568.
9. Liu S, Tang W, Zhou J, et al. Fibroblast growth factor 23 is a counter-regulatory phosphaturic hormone for vitamin D. *J Am Soc Nephrol*. 2006;17(5):1305-1315.
10. Lavi-Moshayoff V, Wasserman G, Meir T, Silver J, Naveh-Many T. PTH increases FGF23 gene expression and mediates the high-FGF23 levels of experimental kidney failure: a bone parathyroid feedback loop. *Am J Physiol Renal Physiol*. 2010;299(4):F882-F889.
11. Antoniucci DM, Yamashita T, Portale AA. Dietary phosphorus regulates serum fibroblast growth factor-23 concentrations in healthy men. *J Clin Endocrinol Metab*. 2006;91(8):3144-3149.
12. David V, Martin A, Isakova T, et al. Inflammation and functional iron deficiency regulate fibroblast growth factor 23 production. *Kidney Int*. 2016;89(1):135-146.
13. Farrow EG, Yu X, Summers LJ, et al. Iron deficiency drives an autosomal dominant hypophosphatemic rickets (ADHR) phenotype in fibroblast growth factor-23 (Fgf23) knock-in mice. *Proc Natl Acad Sci U S A*. 2011;108(46):E1146-E1155.
14. Rabadi S, Udo I, Leaf DE, Waikar SS, Christov M. Acute blood loss stimulates fibroblast growth factor 23 production. *Am J Physiol Renal Physiol*. 2018;314(1):F132-F139.
15. Toro L, Barrientos V, Leon P, et al. Erythropoietin induces bone marrow and plasma fibroblast growth factor 23 during acute kidney injury. *Kidney Int*. 2018;93(5):1131-1141.
16. Hanudel MR, Eisenga MF, Rappaport M, et al. Effects of erythropoietin on fibroblast growth factor 23 in mice and humans. *Nephrol Dial Transplant*. 2019;34(12):2057-2065.
17. Flamme I, Ellinghaus P, Urrego D, Kruger T. FGF23 expression in rodents is directly induced via erythropoietin after inhibition of hypoxia inducible factor proline hydroxylase. *PLoS One*. 2017;12(10):e0186979.
18. Clinkenbeard EL, Hanudel MR, Stayrook KR, et al. Erythropoietin stimulates murine and human fibroblast growth factor-23, revealing novel roles for bone and bone marrow. *Haematologica*. 2017;102(11):e427-e430.
19. Imel EA, Peacock M, Gray AK, Padgett LR, Hui SL, Econs MJ. Iron modifies plasma FGF23 differently in autosomal dominant hypophosphatemic rickets and healthy humans. *J Clin Endocrinol Metab*. 2011;96(11):3541-3549.
20. Clinkenbeard EL, Farrow EG, Summers LJ, et al. Neonatal iron deficiency causes abnormal phosphate metabolism by elevating FGF23 in normal and ADHR mice. *J Bone Miner Res*. 2014;29(2):361-369.
21. Singh S, Grabner A, Yanucil C, et al. Fibroblast growth factor 23 directly targets hepatocytes to promote inflammation in chronic kidney disease. *Kidney Int*. 2016;90(5):985-996.
22. Faul C, Amaral AP, Oskouei B, et al. FGF23 induces left ventricular hypertrophy. *J Clin Invest*. 2011;121(11):4393-4408.
23. Grabner A, Amaral AP, Schramm K, et al. Activation of cardiac fibroblast growth factor receptor 4 causes left ventricular hypertrophy. *Cell Metab*. 2015;22(6):1020-1032.
24. de Las Rivas M, Paul Daniel EJ, Narimatsu Y, et al. Molecular basis for fibroblast growth factor 23 O-glycosylation by GalNAc-T3. *Nat Chem Biol*. 2020;16(3):351-360.
25. Kato K, Jeanneau C, Tarp MA, et al. Polypeptide GalNAc-transferase T3 and familial tumoral calcinosis. Secretion of fibroblast growth factor 23 requires O-glycosylation. *J Biol Chem*. 2006;281(27):18370-18377.
26. Bhattacharyya N, Wiench M, Dumitrescu C, et al. Mechanism of FGF23 processing in fibrous dysplasia. *J Bone Miner Res*. 2012;27(5):1132-1141.
27. Tagliabracci VS, Engel JL, Wiley SE, et al. Dynamic regulation of FGF23 by Fam20C phosphorylation, GalNAc-T3 glycosylation, and furin proteolysis. *Proc Natl Acad Sci U S A*. 2014;111(15):5520-5525.
28. Mehta R, Cai X, Hodakowski A, et al. Fibroblast growth factor 23 and anemia in the chronic renal insufficiency cohort study. *Clin J Am Soc Nephrol*. 2017;12(11):1795-1803.
29. Coe LM, Madathil SV, Casu C, Lanske B, Rivella S, Sitara D. FGF-23 is a negative regulator of prenatal and postnatal erythropoiesis. *J Biol Chem*. 2014;289(14):9795-9810.
30. Ganz T. Hepcidin, a key regulator of iron metabolism and mediator of anemia of inflammation. *Blood*. 2003;102(3):783-788.
31. Truksa J, Peng H, Lee P, Beutler E. Bone morphogenetic proteins 2, 4, and 9 stimulate murine hepcidin 1 expression independently of Hfe, transferrin receptor 2 (Tfr2), and IL-6. *Proc Natl Acad Sci U S A*. 2006;103(27):10289-10293.
32. Lin L, Valore EV, Nemeth E, Goodnough JB, Gabayan V, Ganz T. Iron transferrin regulates hepcidin synthesis in primary hepatocyte culture through hemojuvelin and BMP2/4. *Blood*. 2007;110(6):2182-2189.
33. Andriopoulos B Jr, Corradini E, Xia Y, et al. BMP6 is a key endogenous regulator of hepcidin expression and iron metabolism. *Nat Genet*. 2009;41(4):482-487.
34. Xiao X, Alfaro-Magallanes VM, Babitt JL. Bone morphogenic proteins in iron homeostasis. *Bone*. 2020;138:115495.
35. Simic P, Kim W, Zhou W, et al. Glycerol-3-phosphate is an FGF23 regulator derived from the injured kidney. *J Clin Invest*. 2020;130(3):1513-1526.
36. Roebroek AJ, Taylor NA, Louagie E, et al. Limited redundancy of the proprotein convertase furin in mouse liver. *J Biol Chem*. 2004;279(51):53442-53450.
37. Martin A, David V, Laurence JS, et al. Degradation of MEPE, DMP1, and release of SIBLING ASARM-peptides (minhibins): ASARM-peptide(s) are directly responsible for defective mineralization in HYP. *Endocrinology*. 2008;149(4):1757-1772.
38. Dussold C, Gerber C, White S, et al. DMP1 prevents osteocyte alterations, FGF23 elevation and left ventricular hypertrophy in mice with chronic kidney disease. *Bone Res*. 2019;7:12.
39. Courbon G, Francis C, Gerber C, et al. Lipocalin 2 stimulates bone fibroblast growth factor 23 production in chronic kidney disease. *Bone Res*. 2021;9(1):35.
40. Nemeth E, Ganz T. Anemia of inflammation. *Hematol Oncol Clin North Am*. 2014;28(4):671-681. vi.
41. Kautz L, Jung G, Valore EV, Rivella S, Nemeth E, Ganz T. Identification of erythroferrone as an erythroid regulator of iron metabolism. *Nat Genet*. 2014;46(7):678-684.
42. Czaya B, Heitman K, Campos I, et al. Hyperphosphatemia increases inflammation to exacerbate anemia and skeletal muscle wasting independently of FGF23-FGFR4 signaling. *Elife*. 2022;11:e74782.
43. Bacchetta J, Zaritsky JJ, Sea JL, et al. Suppression of iron-regulatory hepcidin by vitamin D. *J Am Soc Nephrol*. 2014;25(3):564-572.
44. Xiao X, Dev S, Canali S, et al. Endothelial bone morphogenetic protein 2 (Bmp2) knockout exacerbates hemochromatosis in homeostatic iron regulator (Hfe) knockout mice but not Bmp6 knockout mice. *Hepatology*. 2020;72(2):642-655.
45. Canali S, Wang CY, Zumbrennen-Bullough KB, Bayer A, Babitt JL. Bone morphogenetic protein 2 controls iron homeostasis in mice independent of Bmp6. *Am J Hematol*. 2017;92(11):1204-1213.
46. Wang RH, Li C, Xu X, et al. A role of SMAD4 in iron metabolism through the positive regulation of hepcidin expression. *Cell Metab*. 2005;2(6):399-409.
47. Dai B, David V, Martin A, et al. A comparative transcriptome analysis identifying FGF23 regulated genes in the kidney of a mouse CKD model. *PLoS One*. 2012;7(9):e44161.
48. Courbon G, Chonira V, Capella M, et al. C-FGF23 peptide protects against severe hypoferremia during acute inflammation. *J Bone Miner Res*. 2019;34:79.
49. Bansal S, Friedrichs WE, Velagapudi C, et al. Spleen contributes significantly to increased circulating levels of fibroblast growth factor

23 in response to lipopolysaccharide-induced inflammation. *Nephrol Dial Transplant*. 2017;32(6):960-968.

50. Masuda Y, Ohta H, Morita Y, et al. Expression of Fgf23 in activated dendritic cells and macrophages in response to immunological stimuli in mice. *Biol Pharm Bull*. 2015;38(5):687-693.

51. Nakashima Y, Mima T, Yashiro M, et al. Expression and localization of fibroblast growth factor (FGF)23 and Klotho in the spleen: its physiological and functional implications. *Growth Factors*. 2016;34(5-6):196-202.

52. Han X, Li L, Yang J, King G, Xiao Z, Quarles LD. Counter-regulatory paracrine actions of FGF-23 and 1,25(OH)2 D in macrophages. *FEBS Lett*. 2016;590(1):53-67.

53. Lee SM, Carlson AH, Onal M, Benkusky NA, Meyer MB, Pike JW. A control region near the fibroblast growth factor 23 gene mediates response to phosphate, 1,25(OH)2D3, and LPS in vivo. *Endocrinology*. 2019;160(12):2877-2891.

54. Egli-Spichtig D, Zhang MYH, Perwad F. Fibroblast growth factor 23 expression is increased in multiple organs in mice with folic acid-induced acute kidney injury. *Front Physiol*. 2018;9:1494.

55. Wolf M, White KE. Coupling fibroblast growth factor 23 production and cleavage: iron deficiency, rickets, and kidney disease. *Curr Opin Nephrol Hypertens*. 2014;23(4):411-419.

56. Topaz O, Shurman DL, Bergman R, et al. Mutations in GALNT3, encoding a protein involved in O-linked glycosylation, cause familial tumoral calcinosis. *Nat Genet*. 2004;36(6):579-581.

57. Bhattacharyya N, Chong WH, Gafni RI, Collins MT. Fibroblast growth factor 23: state of the field and future directions. *Trends Endocrinol Metab*. 2012;23(12):610-618.

58. Yamamoto H, Ramos-Molina B, Lick AN, et al. Posttranslational processing of FGF23 in osteocytes during the osteoblast to osteocyte transition. *Bone*. 2016;84:120-130.

59. Yuan B, Feng JQ, Bowman S, et al. Hexa-D-arginine treatment increases 7B2*PC2 activity in hyp-mouse osteoblasts and rescues the HYP phenotype. *J Bone Miner Res*. 2013;28(1):56-72.

60. Chen G, Liu Y, Goetz R, et al. Alpha-Klotho is a non-enzymatic molecular scaffold for FGF23 hormone signalling. *Nature*. 2018;553(7689):461-466.

61. Suzuki Y, Kuzina E, An SJ, et al. FGF23 contains two distinct high-affinity binding sites enabling bivalent interactions with alpha-Klotho. *Proc Natl Acad Sci U S A*. 2020;117(50):31800-31807.

62. Urakawa I, Yamazaki Y, Shimada T, et al. Klotho converts canonical FGF receptor into a specific receptor for FGF23. *Nature*. 2006;444(7120):770-774.

63. Agoro R, Montagna A, Goetz R, et al. Inhibition of fibroblast growth factor 23 (FGF23) signaling rescues renal anemia. *FASEB J*. 2018;32(7):3752-3764.

64. Goetz R, Nakada Y, Hu MC, et al. Isolated C-terminal tail of FGF23 alleviates hypophosphatemia by inhibiting FGF23-FGFR-Klotho complex formation. *Proc Natl Acad Sci U S A*. 2010;107(1):407-412.

65. Agoro R, Park MY, Le Henaff C, et al. C-FGF23 peptide alleviates hypoferremia during acute inflammation. *Haematologica*. 2021;106(2):391-403.

66. Johnson K, Levine K, Sergi J, et al. Therapeutic effects of FGF23 c-tail Fc in a murine preclinical model of X-linked hypophosphatemia via the selective modulation of phosphate reabsorption. *J Bone Miner Res*. 2017;32(10):2062-2073.

67. Nicolas G, Bennoun M, Porteu A, et al. Severe iron deficiency anemia in transgenic mice expressing liver hepcidin. *Proc Natl Acad Sci U S A*. 2002;99(7):4596-4601.

68. Eisenga MF, van Londen M, Leaf DE, et al. C-terminal fibroblast growth factor 23, iron deficiency, and mortality in renal transplant recipients. *J Am Soc Nephrol*. 2017;28(12):3639-3646.